J. Phys. B: At. Mol. Opt. Phys. **33** (2000) L127–L133. Printed in the UK PII: S0953-4075(00)10128-2

LETTER TO THE EDITOR

Sequential and nonsequential contributions to double ionization in strong laser fields

Th Weber†, M Weckenbrock†, A Staudte†, L Spielberger†, O Jagutzki†, V Mergel†, F Afaneh†, G Urbasch‡, M Vollmer‡, H Giessen‡ and R Dörner†

† Institut für Kernphysik, Universität Frankfurt, August Euler Straße 6, D-60486 Frankfurt, Germany

‡ Fachbereich Physik, Philipps-Universität, Renthof 5, D-35032 Marburg, Germany

E-mail: Doerner@hsb.uni-frankfurt.de

Received 6 December 1999

Abstract. We demonstrate experimentally the difference between a sequential interaction of a femtosecond laser field with two electrons and a nonsequential process of double ionization mediated by electron–electron correlation. This is possible by observing the momentum distribution of doubly charged argon ions created in the laser field. In the regime of laser intensities where the nonsequential process dominates, an increase in laser power leads to an increase in the observed ion momenta. At the onset of the sequential process, however, a higher laser power leads to colder ions. The momentum distributions of the ions from the sequential process can be modelled by convolving the single-ionization distribution with itself.

Coupling of a time-dependent field to a quantum mechanical many-body Coulomb system can lead to two-body transitions in at least two ways. One way is an independent coupling of the external field to each of the two particles that are to be excited. The other way is the interaction of a single particle, which then excites the second particle by correlation within the composed system. Prominent examples for such behaviour can be found in atomic physics if two electrons in an atom are ejected by time-dependent fields, for example, from an intense laser or a traversing charged particle. Generally, the contribution due to two interactions with the field decreases much faster with decreasing perturbation strength than the process involving internal correlation. For double ionization by a short (femtosecond) intense laser (10^{14}–10^{16} W cm^{-2}), the process involving two interactions with the field is referred to as sequential double ionization (see, e.g., [1, 2] and [3] for a recent review), while for charged particle impact it is commonly called TS2 (two step two) (see, e.g., [4, 5] and [6] for a recent review).

For laser impact, the distinction of the sequential and nonsequential double-ionization mechanisms is so far based solely on the experimental observation of a stepwise increase of the ratio (R) of the rates of doubly-to-singly charged ions with increasing perturbation strength and its theoretical interpretation (see [1, 2] for experiments on helium and [7, 8] for experiments on argon and other noble gas targets (cf also [9]). Theoretically, a clear cut distinction between the sequential and nonsequential process can be made in terms of Feynman diagrams [9, 10]. Recently, Dundas and co-workers have analysed sequential and nonsequential contributions in an elaborate three-dimensional time-dependent calculation [11]. The main finding of an

intermediate regime where double ionization is dominantly mediated by electron–electron correlation, has been confirmed by numerous model calculations (see, e.g., [12–19] and [3] for a recent review).

In this letter we show experimentally that the nonsequential process leads to a different momentum distribution for the doubly charged ions if compared with the sequential process. Recently Moshammer and co-workers and our collaboration have reported such an ionic momentum distribution for an Ne target [20] and He targets [21]. Both studies, however, were performed at too low laser intensities where the sequential process is negligible. For this letter we choose argon as a target, since here the sequential process sets in at intensities accessible to our laser system.

We employed the well established technique of COLTRIMS (cold-target recoil-ion momentum spectroscopy) (see [22, 23] for recent reviews). A supersonic gas jet provided sufficiently cold target atoms to allow for a measurement of the rather small (subthermal) ionic momenta. The linearly polarized light of a Ti:sapphire laser at 800 nm (Spectra-Physics Spitfire) with a pulse width of 220 fs, and a repetition rate of 1 kHz was focused by a 5 cm lens onto the gas jet. The focal diameter was about 7 μm. The ions created at the focus are accelerated by a homogeneous electric field of 4 V cm^{-1} followed by a field-free drift region onto a position-sensitive channel-plate detector. A figure depicting our set-up can be found in [24]. From the time of flight and the position of impact on the detector the charge state and momentum vector of the ion can be determined. The resolution is mainly restricted by the temperature of the gas jet. From an electron–ion coincidence detection for single ionization we found a resolution of about 0.3 au for the ion momentum in the direction of polarization, which coincides with the direction of the extraction field of the spectrometer. The peak laser power was determined by fitting our He^+ ion yields, measured over five orders of magnitude as a function of the integral laser power to ion yield calculations of Becker (adapted to the present conditions from [9]). We estimate the accuracy of this calibration to be approximately 15%.

The ratio of the Ar^{2+} and Ar^+ rates as a function of the laser peak power (figure 1) shows the well established steep increase starting at a power of about 4–5 $\times 10^{14}$ W cm^{-2}. For comparison, data from [7] (small dots) and [8] and results of an *S*-matrix calculation by Becker and Faisal [9] are shown. All data show the steep rise in the ratio. The most probable reason for the difference in the absolute height are uncertainties in the determination of the laser peak power. The recoil-ion momentum distribution at five different peak intensities indicated by labels (*a*)–(*e*) in figure 1 are shown in figure 2. We find the momentum distribution of the Ar^{2+} ions to be aligned along the electric field vector of the light (horizontal). For intensities of 2×10^{14} and 3.75×10^{14} W cm^{-2} the momenta in the field direction increase with peak power. This is similar to our observations for a helium target [21]. At 3.75×10^{14} W cm^{-2}, a flat top on the momentum distribution is found (figures 2(*b*) and (*g*)). For helium [21] and neon [20] targets, a further increase of laser power leads from a flat top to a minimum at the momentum zero. For an argon target, however, a narrow peak on top of the flat-top distribution arises at intensities above 6×10^{14} W cm^{-2} (figure 2(*c*)). The appearance of these low momentum ions corresponds to an increase of approximately 40% in the ratio of doubly-to-singly charged ions. With a further increase in laser power, the narrow peak close to zero momentum dominates the distribution (figures 2(*d*) and (*e*)). Thus higher optical fields yield much colder ions. This change in the momentum distribution is accompanied by the sharp rise of the ratio Ar^{2+}/Ar^+. The observed dramatic change in the ionic momentum distributions indicates the transition from nonsequential to sequential ionization as we will explain in the following.

To model the momentum distribution resulting from the sequential process, we have convolved the measured momentum distribution for Ar^+ ions with itself. The chain curve in

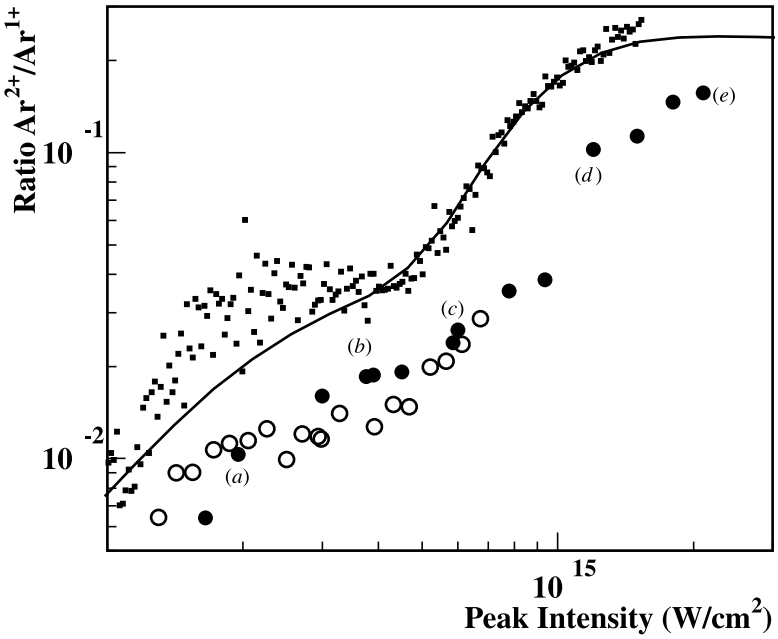

Figure 1. Ratio Ar^{2+}/Ar^{+} of rates of doubly-to-singly charged argon ions created in the focus of an 800 nm laser pulse as a function of the peak intensity. The full curve shows an *S*-matrix calculation by Becker and Faisal adapted to the present laser conditions [9]. Small dots, from [7] (200 fs); open circles, from [8] (30 fs); large full circles, this work (220 fs). The labels (*a*)–(*e*) indicate the points for which the momentum distribution of the Ar^{2+} ions is shown in figures 2(*a*)–(*e*).

figure 3 shows the measured momentum distribution of Ar^{+} ions and the broken curve the autocorrelated one. Thus the broken distribution is the chain one convolved with itself. This convolution was performed by adding the momentum vectors of two independent Ar^{+} ions from different laser pulses. This assumes that the ejection of the two electrons can be regarded as two uncorrelated events, spaced in time by a random number of optical cycles. Figure 3 shows that at 12×10^{14} W cm^{-2} this very simple approach describes the double ionization rather well, while it fails completely at 3.75×10^{14} W cm^{-2} and lower intensities.

For single ionization, the ionic momentum distribution is a mirror image of the electronic momentum distribution, since the pulse is short enough to prohibit the electrons from leaving the focus during that time. For double ionization, the ionic momenta mirror the vector sum of both electron momenta. The success of our simple convolution model shows that there is no significant angular or energetic correlation between the two electrons at high intensities.

One obvious oversimplification of our convolution procedure is that it implicitly assumes that the momentum distributions do not change with binding energy. For single ionization, the relevant binding energy is 24 eV. By modelling the sequential process by convolving the Ar^{+} distribution with itself, one neglects the fact that the removal of the second electron requires 54 eV. Clearly, this unrealistic assumption does not allow one to predict the overall Ar^{2+} rate. A more refined independent electron approach could use different binding energies for both steps. As an alternative simple model, we have calculated the momentum distributions for removal of the first electron and the second electron in the Ammosov–Delone–Krainov (ADK) model (see, e.g., [25], equation (10)) using the correct binding energies for both steps. The result of convolving these two calculated distributions is shown by the full curves in figure 3.

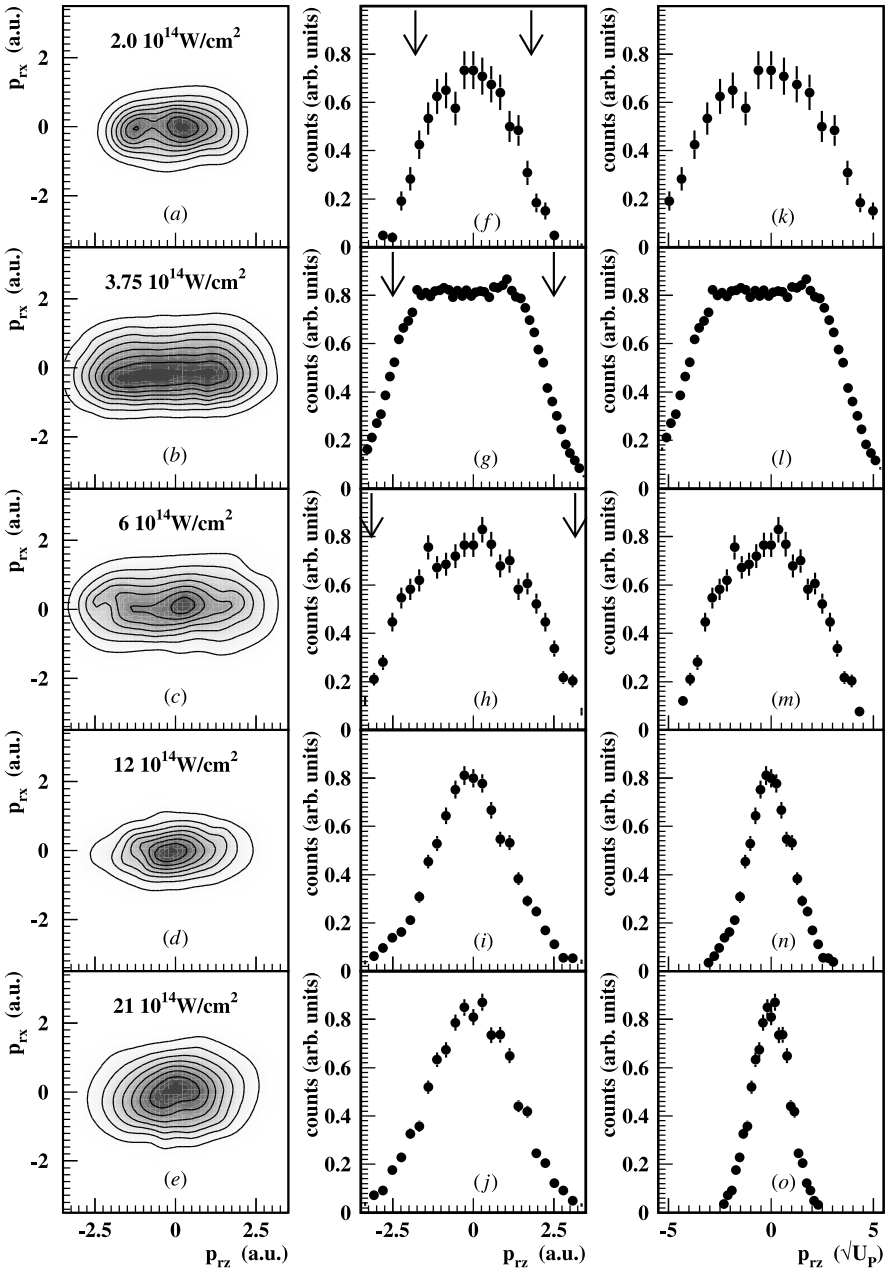

Figure 2. Momentum distribution of Ar^{2+} ions created in the focus of a 220 fs, 800 nm laser pulse at peak intensities of 2×10^{14} W cm^{-2} (*a*), (*f*) and (*k*), 3.75×10^{14} W cm^{-2} (*b*), (*g*) and (*k*), 6×10^{14} W cm^{-2} (*c*), (*h*) and (*m*), 12×10^{14} W cm^{-2} (*d*), (*i*) and (*n*), 21×10^{14} W cm^{-2} (*e*), (*j*) and (*o*) and linear polarization (see labels in figure 1). The horizontal axis shows the momentum component along the electric field vector (p_{zr}), the vertical axis is the momentum component in the direction of the light propagation (p_{xr}). The distribution is integrated over p_{yr}. The curves show levels of equal count rate on a linear scale. The middle row (*f*)–(*j*) shows projections of the two-dimensional distributions on the right-hand row onto the horizontal axis (direction of polarization). Right row (*k*)–(*o*): same data as the middle row, the horizontal axis is in units of the ponderomotive momentum $\sqrt{U_P}$ (see text).

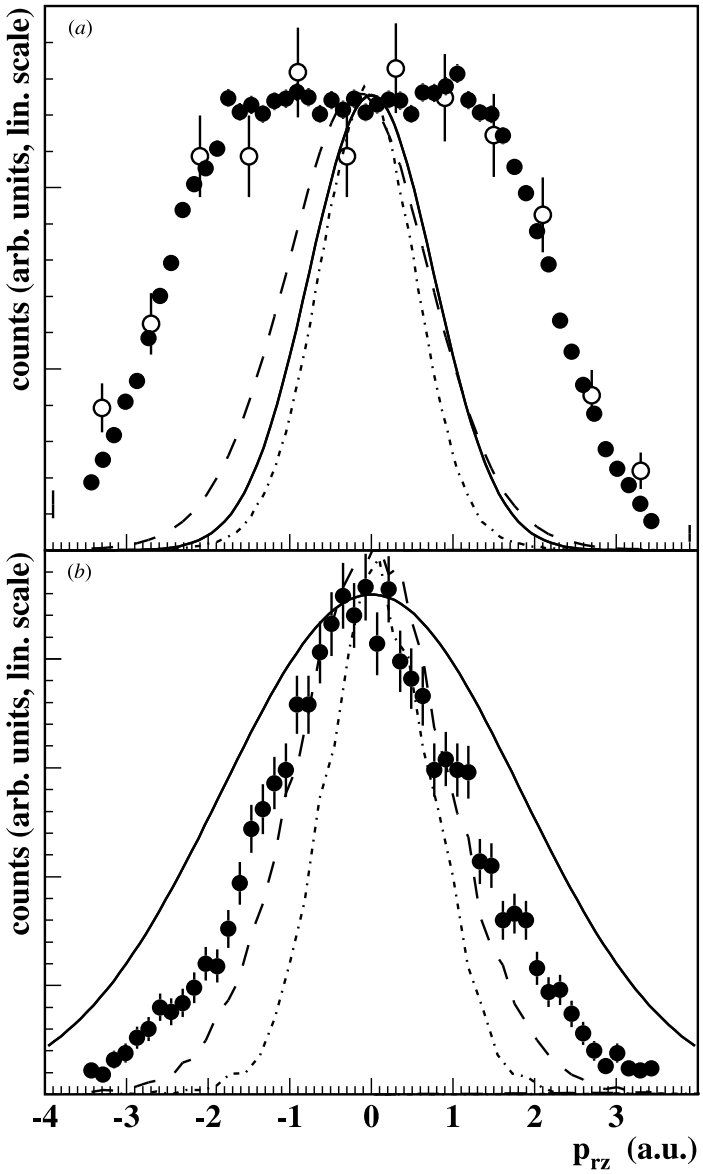

Figure 3. Momentum distribution of Ar^{2+} ions created at the focus of a 220 fs, 800 nm laser pulse at peak intensities of (*a*) 3.75×10^{14} W cm^{-2} and (*b*) 12×10^{14} W cm^{-2} in the direction of polarization. The distributions are integrated over the directions perpendicular to the polarization. The full circles show the distribution of Ar^{2+} ions (same as in figures 2(*g*) and (*i*)). Chain curve, distribution of Ar^{+} ions; broken curve, results of the independent electron model of convolving the Ar^{+} distribution with itself; and full curve, independent electron ADK model (see text). The open circles in (*a*) show the distribution of He^{2+} ions at 3.8×10^{14} W cm^{-2} (from [21]).

Furthermore, at 3.75×10^{14} W cm^{-2} (nonsequential regime), the momentum distribution of the Ar^{2+} ions (full circles in figure 3(*a*)) are within the error bars identical to the distribution of He^{2+} [21] ions (open symbols) at a similar intensity. This indicates that the double-ionization mechanism in this intensity regime is the same for helium and argon, even though the ratio

of double-to-single ionization is as different as 0.049% and 2.6%. The similarity of the Ar^{2+} and He^{2+} momenta supports the assumption that these momenta in the direction of the polarization are mainly a result of the acceleration of the ions in the laser field and are not being determined by the initial state of the atom. The momentum transfer from the laser field depends only on the phase at which the ion is created and on its charge but not on its mass.

The maximum momentum a doubly charged particle can acquire in an optical field is given by $p_z = 4\sqrt{U_P}$, where $U_P = 2\pi I/c\omega^2$ is the ponderomotive energy, i.e. the mean quiver energy of a free electron in the photon field of frequency ω and intensity I (in atomic units). This momentum is indicated by the arrows in figure 2. It corresponds to an ion which is created with charge two at the time when the optical field crosses zero. To allow for an easier comparison between the distributions at the different intensities the momenta are shown in units of $\sqrt{U_P}$ in the right-hand column of figure 2. In this representation the trivial increase of momenta due to the rise of the quiver momentum does not occur and the influence of the change in the physical mechanism becomes more prominent.

In conclusion, we have given direct experimental support for the common interpretation of two different mechanisms for multiphoton double ionization. The nonsequential mechanism leads to much larger ion momenta compared with the sequential process. For argon, the momentum distributions of doubly charged ions from the sequential and the nonsequential process have very different shapes. However, the distributions overlap in momentum space. For helium and neon, the sequential process becomes significant at much higher intensities, at which the momentum distributions for the nonsequential process have evolved from a flat-top distribution to a two-peak structure with a minimum at zero momentum (see [20, 21]). Therefore, we expect that for these targets the sequential process will manifest itself in a third, distinct peak at momentum zero in the momentum distributions.

We are indebted to Horst Schmidt-Böcking for enthusiastic support of this project and to Andreas Becker, Farhad Faisal, Robert Moshammer and Joachim Ullrich for many helpful discussions. We thank S L Chin for communication of their data in electronic form. This work is supported by DFG, BMBF, GSI and DAAD. RD acknowledges supported by the Heisenberg-Programme of the DFG. The Marburg group thanks the DFG for support through their SFB383 and their Graduiertenkolleg 'Optoelektronik mesoskopischer Halbleiter'. We acknowledge expert technical assistance by H Fries. We are grateful to W W Rühle for continuous support.

References

[1] Fittinghoff D N, Bolton P R, Chang B and Kulander K D 1992 *Phys. Rev. Lett.* **69** 2642
[2] Walker B, Sheehy B, DiMauro L F, Agostini P, Schafer K H and Kulander K C 1994 *Phys. Rev. Lett.* **73** 1227
[3] Lambropoulos P, Maragakis P and Zhang J 1998 *Phys. Rep.* **305** 203
[4] Ullrich J *et al* 1993 *Phys. Rev. Lett.* **71** 1697
[5] Andersen L H, Hvelplund P, Knudsen H, Moller S P, Pedersen J O P, Tang-Pedersen S, Uggerhoj E, Elsener K and Morenzoni E 1989 *Phys. Rev.* A **40** 7366
[6] McGuire J H 1997 *Electron Correlation Dynamics in Atomic Collisions* (Cambridge: Cambridge University Press)
[7] Larochelle S, Talebpour A and Chin S L 1998 *J. Phys. B: At. Mol. Opt. Phys.* **31** 1201
[8] Guo C, Li M, Nibarger J P and Gibson G N 1998 *Phys. Rev.* A **58** R4271
[9] Becker A and Faisal F H M 1999 *J. Phys. B: At. Mol. Opt. Phys.* **32** L335
[10] Becker A and Faisal F H M 1999 *Phys. Rev.* A **59** R1742
[11] Dundas D, Taylor K T, Parker J and Smyth E 1999 *J. Phys. B: At. Mol. Opt. Phys.* **32** L231
[12] Liu W C, Eberly J H, Haan S L and Grobe R 1999 *Phys. Rev. Lett.* **83** 520

[13] Watson J B, Sanpera A, Lappas D G, Knight P L and Burnett K 1997 *Phys. Rev. Lett.* **78** 1884
[14] Kuchiev M Yu 1995 *J. Phys. B: At. Mol. Opt. Phys.* **28** 5093
[15] Lappas D G and van Leeuwen R 1998 *J. Phys. B: At. Mol. Opt. Phys.* **31** L249
[16] Lein M, Gross E K U and Engel V 2000 *J. Phys. B: At. Mol. Opt. Phys.* **33** 433
[17] LaGattuta K J and Cohen J S 1998 *J. Phys. B: At. Mol. Opt. Phys.* **31** 5281
[18] Corkum P B 1993 *Phys. Rev. Lett.* **71** 1994
[19] Kulander K C, Cooper J and Schafer K J 1995 *Phys. Rev.* A **51** 561
[20] Moshammer R *et al* 2000 *Phys. Rev. Lett.* **84** 447
[21] Weber Th, Weckenbrock M, Staudte A, Spielberger L, Jagutzki O, Mergel V, Urbasch G, Vollmer M, Giessen H and Dörner R 2000 *Phys. Rev. Lett.* **84** 443
[22] Dörner R, Mergel V, Jagutzki O, Spielberger L, Ullrich J, Moshammer R and Schmidt-Böcking H 2000 *Phys. Rep.* at press
[23] Ullrich J, Moshammer R, Dörner R, Jagutzki O, Mergel V, Schmidt-Böcking H and Spielberger L 1997 *J. Phys. B: At. Mol. Opt. Phys.* **30** 2917
[24] Mergel V *et al* 1995 *Phys. Rev. Lett.* **74** 2200
[25] Delone N B and Krainov V P 1998 *Phys. Usp.* **41** 469